Structure and breakdown properties of polypropylene-based nanocomposites

Structure and Breakdown Properties of Polypropylene-based Nanocomposites

A.Azmi
School of Electrical Engineering
Universiti Teknologi Malaysia
Johor Bahru, Malaysia
aizat.azmi.1987@gmail.com

K. Y. Lau
School of Electrical Engineering
Universiti Teknologi Malaysia
Johor Bahru, Malaysia
kwanyiew@utm.my

N. A. Ahmad
School of Electrical Engineering
Universiti Teknologi Malaysia
Johor Bahru, Malaysia
noorazlinda@utm.my

Z. Abdul-Malek
School of Electrical Engineering
Universiti Teknologi Malaysia
Johor Bahru, Malaysia
zulkurnain@utm.my

C. W. Tan
School of Electrical Engineering
Universiti Teknologi Malaysia
Johor Bahru, Malaysia
cheewei@fke.utm.my

K. Y. Ching
School of Foundation
University of Reading Malaysia
Iskandar Puteri, Malaysia
k.y.ching@reading.edu.my

***Abstract*— This work was performed to investigate the effects of different nanofillers on the structure and dielectric properties of polypropylene (PP) nanocomposites. This work considered studying three types of nanofillers, namely, magnesium aluminate ($MgAl_2O_4$), calcium carbonate ($CaCO_3$), and surface-modified calcium carbonate ($CaCO_3T$). PP nanocomposites containing $MgAl_2O_4$, $CaCO_3$, and $CaCO_3T$ nanofillers were prepared using a Brabender melt mixer. The samples were melt pressed using a hydraulic laboratory press at 180 °C to produce thin-film samples of 100 µm thick. The prepared samples were subjected to Fourier transform infrared (FTIR) spectroscopy and scanning electron microscopy (SEM) for chemical and morphological analysis. Meanwhile, the DC breakdown test was carried out to analyzed the dielectric properties of the evaluated samples. The results showed that PP/$MgAl_2O_4$ nanocomposites possessed lowered breakdown strength compared to unfilled PP. In contrast, PP/$CaCO_3$ nanocomposites possessed a higher breakdown strength over PP/$MgAl_2O_4$ nanocomposites. Meanwhile, PP/$CaCO_3T$ nanocomposites possessed the highest breakdown strength among the nanocomposites. Possible mechanisms governing these property changes are discussed.**

Keywords—nanocomposites, polypropylene, magnesium aluminate, calcium carbonate, breakdown

I. INTRODUCTION

Polypropylene (PP) material has a huge potential to be used as a high voltage cable insulation. Previous research shows that PP is thermally stable and could be operated at high-temperature conditions [1-3]. This was mainly due to its characteristics such as having high melting temperature, low dielectric constant, and high mechanical strength and reduced space charge accumulation. Besides that, PP is classified as a thermoplastic material that can easily be recycled compared to the conventional cross-linked polyethylene (XLPE) cable insulation.

Currently, single metal oxide nanofillers have been added to PP to improve the dielectric properties of the resulting systems [4-6]. For example, Cao et al. [7] found that the addition of magnesium oxide (MgO) into PP has restricted the electric field distortion and space charge accumulation within the PP nanocomposites. In addition, the DC breakdown strength of PP nanocomposites improved when added with low amount of MgO. Similarly, Zhou et al. [8] revealed that the addition of titanium dioxide (TiO_2), zinc oxide (ZnO), and aluminum oxide (Al_2O_3) to PP enhanced the DC breakdown strength of PP nanocomposites. Besides that, those nanoparticles have also improved the DC volume resistivity, permittivity, and space charge behavior of PP nanocomposites. A similar observation was reported by Zha et al. [9] where ZnO nanofiller led to the improvement in DC breakdown strength, reduced space charge, and mechanical properties of PP nanocomposites. Meanwhile, Mirjalili et al. [10] discovered the enhancement in the mechanical properties of PP when introduced Al_2O_3 nanofiller. Of note, all of these reports show that the respective nanofiller has been well dispersed in the polymer, thus improving the dielectric properties of the materials.

The water shell phenomenon or much related to water absorption is a common problem for nanocomposites containing single metal oxide nanofillers. Water absorption on the single metal oxide nanofillers would degrade the nanocomposites by lowering the breakdown strength [11-12]. Recently, multi-element oxide nanofillers have shown unique characteristics such as having a compact structure with supreme thermal, mechanical, and electrical properties compared to single-metal oxide nanofillers [13-14]. Samad et al [15] found that polyethylene (PE) nanocomposites containing magnesium aluminate ($MgAl_2O_4$) had greater breakdown strength than that of PE containing Al_2O_3. Meanwhile, Virtanen et al [13] reported that calcium carbonate ($CaCO_3$) with 150 nm in size and homogeneously well dispersed has increased the DC breakdown strength of PP. Besides that, the addition of $CaCO_3$ has improved the thermal stability of PP [16-17] and poly(vinylidene fluoride) (PVDF) [18]. Lin et al. [19] demonstrated that the crystallization temperature of PP nanocomposites increased with the $CaCO_3$ nanofiller loading level. Similar observation was reported by Fuad et al. [20]. Generally, the improvement in thermal, mechanical, and electrical properties was led by a high specific surface area possesses by the $CaCO_3$ nanofiller. Although the use of multi-element oxide nanofillers in nanocomposites seems promising, the application of such nanofillers is less well explored from the perspective of nanocomposite dielectrics.

Therefore, it is important to study the effect of different multi-element oxide nanofillers on the dielectric properties of PP. In this work, three different types of multi-element oxide nanofillers, i.e., $MgAl_2O_4$, $CaCO_3$, and surface-modified $CaCO_3$ nanofillers, were considered. The developed nanocomposites were characterized and tested by means of scanning electron microscopy (SEM), Fourier transforms infrared (FTIR) spectroscopy, and DC breakdown testing.

978-1-7281-8238-4/21/$31.00 ©2021 IEEE

II. RESEARCH METHOD

A. Sample Preparation

The PP used was a PP blend composed of 50% PP homopolymer and PP impact copolymer. The product grade of these PPs were TITANPRO 6531M and TITANPRO SM340, respectively, and were obtained from Lotte Chemical Titan. Besides that, $MgAl_2O_4$ nanofiller was obtained from Sigma Aldrich. According to the manufacturer, $MgAl_2O_4$ has a size of less than 50 nm. Meanwhile, $CaCO_3$ and $CaCO_3T$ (surface modified) were obtained from SkySpring Nanomaterials. The obtained calcium carbonate has a particle size of 15-40 nm. 1, 2, and 5 wt% of nanofiller loading levels were chosen. PP nanocomposites containing $MgAl_2O_4$, $CaCO_3$, and $CaCO_3T$ were prepared by using a Brabender melt mixer. The temperature, rotational speed, and duration were set at 180 °C, 50 rpm, and 10 min, respectively. The hydraulic laboratory press was used to obtain thin-film samples with 100 µm in thickness. The temperature and pressure were set to 180 °C and 3 ton, respectively. The melt pressed samples were then left to cool down naturally under laboratory ambient conditions. For convenience, all samples were designated using the general notation "P/F/A". In this, P refers to the polymers, F signifies the nanofiller type, and A represents the amount, as indicated in Table I.

B. Scanning Electron Spectroscopy

The morphological structure and dispersion state of the $MgAl_2O_4$, $CaCO_3$, and $CaCO_3T$ within PP were obtained using Hitachi TM3000 SEM. As such, the voltage and working distance were set to 15 kV and 38 mm, respectively. The fracture surfaces of the samples were then sputter-coated with platinum using Quorum SC 7620 automated platinum sputter coater at 15-18 mA for 1 min to minimize charge accumulation and poor resolution during SEM.

C. Fourier transforms infrared

Fourier transform infrared (FTIR) spectroscopy (Shimadzu spectrometer model IRTracer-100) was used to obtain chemical information pertaining to the materials. Thin-film samples (nominally 100 µm in thickness) were characterized for this purpose and the spectral data were collected from 500 to 4000 cm^{-1} over 8 scans at 4 cm^{-1} resolution.

D. Electrical Breakdown

DC breakdown tests were performed using a dielectric strength tester. The schematic diagram of the experimental setup for the DC breakdown strength test is illustrated in Fig. 1. The thickness of each test sample was approximately 100 µm. The samples were sandwiched between two steel ball electrodes and were immersed in mineral oil to prevent surface flashover. A DC step voltage of 2 kV every 20 s was applied until breakdown. 15 breakdown points were recorded for each sample type, and the breakdown

TABLE I. SAMPLE DESIGNATION

Samples (P/F/A)	Polymer (P)	Filler (F)	Amount (A)
PP/0/0	PP	No filler	0 wt%
PP/$MgAl_2O_4$/1	PP	$MgAl_2O_4$	1 wt%
PP/$MgAl_2O_4$/2	PP	$MgAl_2O_4$	2 wt%
PP/$MgAl_2O_4$/5	PP	$MgAl_2O_4$	5 wt%
PP/$CaCO_3$/1	PP	$CaCO_3$	1 wt%
PP/$CaCO_3$/2	PP	$CaCO_3$	2 wt%
PP/$CaCO_3$/5	PP	$CaCO_3$	5 wt%
PP/$CaCO_3T$/1	PP	$CaCO_3T$	1 wt%
PP/$CaCO_3T$/2	PP	$CaCO_3T$	2 wt%
PP/$CaCO_3T$/5	PP	$CaCO_3T$	5 wt%

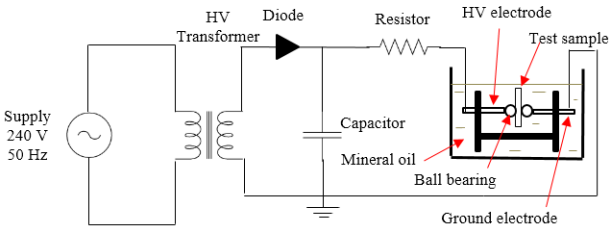

Fig. 1. Schematic diagram illustrating the experimental setup for DC breakdown test

data were analyzed using the two-parameter Weibull distribution.

III. RESULTS AND ANALYSIS

A. Fourier Transformed Infrared Spectroscopy

The FTIR spectra of $MgAl_2O_4$, $CaCO_3$, and $CaCO_3T$ nanopowders are presented in Fig.2. It can be observed that $MgAl_2O_4$ has two absorption bands located at 686 cm^{-1} and 526 cm^{-1}. These absorption bands are indicative of the stretching vibration of MgO_4 tetrahedral and AlO_6 octahedralgroups, respectively. Besides that, a weak absorption band at about 3400 cm^{-1} can be observed, which representing the presence of surface hydroxyl groups and related water molecules on $MgAl_2O_4$ [4]. Meanwhile, $CaCO_3$ and $CaCO_3T$ show three absorption bands. Specifically, those absorption bands located at 1418 cm^{-1}, 873 cm^{-1}, and 707 cm^{-1} spectra, which are indicative of the fundamental bands of the calcite structure and asymmetrical stretching vibration peaks of O-C-O.

The FTIR spectra of the unfilled PP and PP nanocomposites containing 1, 2, and 5 wt% of $MgAl_2O_4$, $CaCO_3$, and $CaCO_3T$ are shown in Fig. 3. For the unfilled PP, the absorption peaks between 2836 cm^{-1} and 2950 cm^{-1} representing the stretching vibration of methyl and methylene groups. Meanwhile, the absorption peaks from 844 cm^{-1} to 1458 cm^{-1} show the bending vibration of methyl and methylene groups. By adding $MgAl_2O_4$ nanofiller into PP, a characteristic absorption peak of $MgAl_2O_4$ at 686 cm^{-1} (as discussed previously) can be observed, and the peak becomes more apparent with increasing $MgAl_2O_4$ loading. Meanwhile, the addition of $CaCO_3$ and $CaCO_3T$ to PP results in additional absorption bands that belong to the nanofillers at 873 cm^{-1} and 707 cm^{-1}. These demonstrate the successful addition of $MgAl_2O_4$, $CaCO_3$, and $CaCO_3T$ to PP.

B. Scanning Electron Spectroscopy

Fig. 4. shows the SEM micrograph of unfilled PP and PP nanocomposites containing $MgAl_2O_4$, $CaCO_3$, and $CaCO_3T$ to PP. The SEM micrograph of the unfilled PP as demonstrated

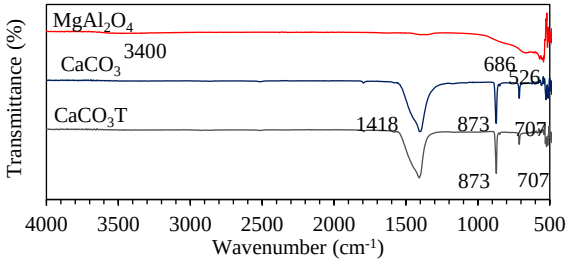

Fig. 2. FTIR spectra of $MgAl_2O_4$, $CaCO_3$, and $CaCO_3T$ nanopowders.

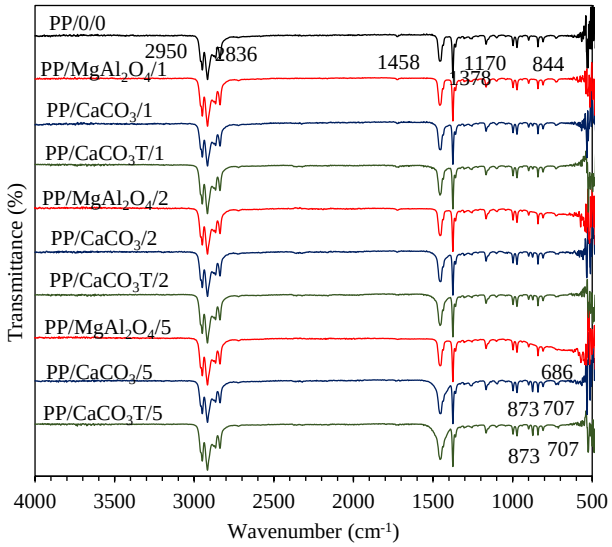

Fig. 3. FTIR spectra comparing unfilled PP and nanocomposites containing 5 wt% of $MgAl_2O_4$, $CaCO_3$, and $CaCO_3T$.

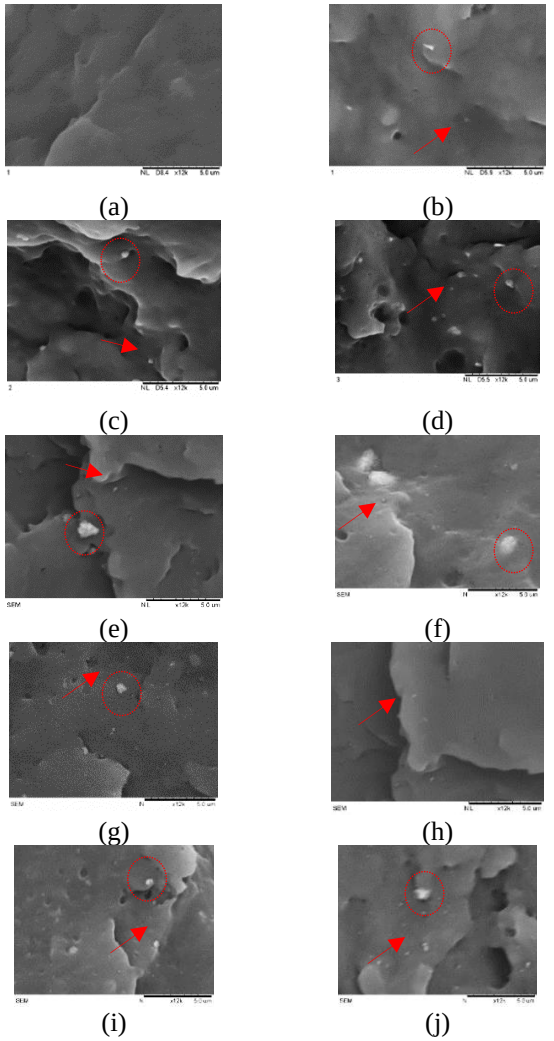

Fig. 4. SEM micrograph of (a) PP/0/0, (b) PP/$MgAl_2O_4$/1, (c) PP/$MgAl_2O_4$/2, (d) PP/$MgAl_2O_4$/5, (e) PP/$CaCO_3$/1, (f) PP/$CaCO_3$/2 (g) PP/$CaCO_3$/5, (h) PP/$CaCO_3T$/1, (i) PP/$CaCO_3T$/2, and (j) PP/$CaCO_3T$/5

in Fig. 4a shows that there was no phase separation in this system. Nevertheless, the structure of this system is not well revealed. Meanwhile, Fig. 4b, 4c, and 4d show SEM images of nanocomposites containing 1, 2, and 5 wt% of $MgAl_2O_4$. Significantly, good dispersion of $MgAl_2O_4$ down to ~100 nm can be observed (arrowed), albeit that some agglomeration of $MgAl_2O_4$ is present (circled). Of note, the agglomeration appears more apparent with increasing $MgAl_2O_4$ (compare Fig. 4b and Fig. 4d). Besides that, Fig. 4e, 4f, and 4g show the SEM morphology of nanocomposites containing 1, 2, and 5 wt% of $CaCO_3$, respectively. Figures 4h, 4i, and 4j contain equivalent images obtained from nanocomposites containing 1, 2, and 5 wt% of $CaCO_3T$, respectively. Again, good dispersion of $CaCO_3$ and $CaCO_3T$ down to ~100 nm can be observed. With a modified nanofiller surface, better $CaCO_3T$ dispersion in PP can be observed compared to $MgAl_2O_4$ and $CaCO_3$. The agglomeration of nanoparticles is well known to be one of the dominant factors that affect the dielectric properties of nanocomposites. SEM analysis suggests that nanocomposites containing $CaCO_3T$ contain more small particles compared to nanocomposites containing $MgAl_2O_4$ and $CaCO_3$.

C. Electrical Breakdown

Fig. 5. compares the DC breakdown strength of unfilled PP and nanocomposites containing 1, 2, and 5 wt% of $MgAl_2O_4$, $CaCO_3$, and $CaCO_3T$ nanofillers; derived Weibull parameters are listed in Table II. The DC breakdown strength of unfilled PP was 323±18 kV mm^{-1}. By adding 1 wt% of $MgAl_2O_4$ to PP, the DC breakdown strength was reduced to 218 ± 10 kV mm^{-1}. A further reduction in the DC breakdown strength is observed when added 2 wt% and 5 wt% of $MgAl_2O_4$ to PP. Meanwhile, adding 1 wt% of $CaCO_3$, the breakdown strength increased to 275±11 kV mm^{-1} and further increased to 300±7 kV mm^{-1} when added 1 wt% of $CaCO_3T$ into PP. Similarly, the DC breakdown strength of PP nanocomposites containing $CaCO_3$ and $CaCO_3T$ was reduced at higher nanofiller loading levels. This result shows that agglomeration can cause severe effects on the DC breakdown strength of the evaluated samples. Besides that, the much lower DC breakdown strength possesses by PP nanocomposites containing $MgAl_2O_4$ was also contributed by the presence of water. According to Guo *et al.* [21], the presence of water within the nanocomposites enhanced the electrical conduction, which subsequently leads to a reduction in the DC breakdown strength [22].

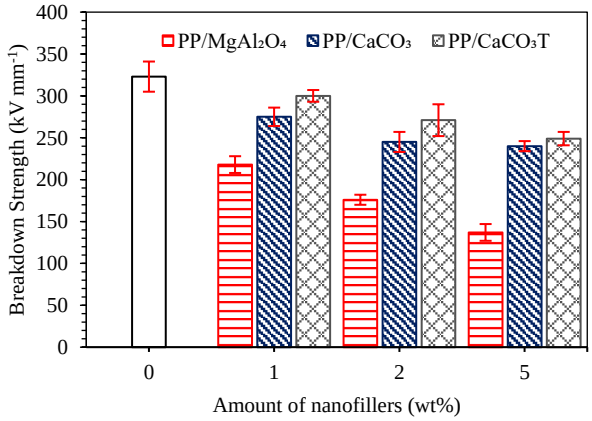

Fig. 5. DC breakdown strength comparing unfilled PP with PP nanocomposites containing $MgAl_2O_4$, $CaCO_3$, and $CaCO_3T$, respectively

TABLE II. DC BREAKDOWN PARAMETERS

Sample	α (kVmm^{-1})	β
PP/0/0	323 ± 18	17 ± 8
PP/$MgAl_2O_4$-1/0	218 ± 10	10 ± 4
PP/$CaCO_3$-1/0	275 ± 11	11±4
PP/$CaCO_3$T-1/0	300 ± 7	20 ± 7
PP/$MgAl_2O_4$-2/0	176 ± 6	13 ± 5
PP/$CaCO_3$-2/0	245 ± 12	9 ± 3
PP/$CaCO_3$T-2/0	271 ± 19	7 ± 2
PP/$MgAl_2O_4$-5/0	137 ± 10	7 ± 3
PP/$CaCO_3$-5/0	240 ± 6	13 ± 3
PP/$CaCO_3$T-5/0	249 ± 8	14 ± 6

Zha et al. [11] stated that the conductivity of nanocomposites has a proportional relationship with nanofiller content. For instance, a low amount of nanofiller added to the polymer provides low conductivity of the nanocomposites. The lower conductivity, in return, improve the DC breakdown strength. On the other hand, the agglomeration of the nanofiller will introduce impurities in the polymer. The ionization of impurities promotes the concentration of free electrons. Hence, reduced the breakdown strength.

IV. CONCLUSIONS

The current work reports on the effects of different multi-element oxide nanofillers on the dielectric properties of PP The observed reduction in the DC breakdown strength of the investigated $MgAl_2O_4$, $CaCO_3$, and $CaCO_3T$ based nanocomposites with increasing nanofiller loading levels is associated with the agglomeration of the nanofiller. Besides that, the much lower DC breakdown of PP nanocomposites containing $MgAl_2O_4$ was due to water absorption on the $MgAl_2O_4$ nanofiller. The increase in the DC breakdown of PP nanocomposites containing $CaCO_3T$ was attributed to the fine and homogeneously distributed nanofillers in PP.

ACKNOWLEDGMENTS

The authors thank the Malaysia Ministry of Education, Universiti Teknologi Malaysia, and Nippon Sheet Glass Foundation for Materials Science and Engineering for financial sponsorship and the respective Fundamental Research Grant Scheme (FRGS/1/2019/TK04/UTM/02/1 (5F158)), RUG (16J55), and NSG (4B373) research grants. Scholarship from UTM Zamalah PhD is also acknowledged.

REFERENCES

[1] K. Kurahashi, Y. Matsuda, A. Ueda, T. Demura, Y. Miyashita, and K. Yoshino, "The Application of Novel Polypropylene to the Insulation of Electric Power Cable."

[2] I. L. Hosier, L. Cozzarini, A. S. Vaughan, and S. G. Swingler, "Propylene based systems for high voltage cable insulation applications," in *Journal of Physics: Conference Series*, 2009, vol. 183.

[3] Y. Zhou, J. He, J. Hu, X. Huang, and P. Jiang, "Evaluation of Polypropylene/Polyolefin Elastomer Blends for Potential Recyclable HVDC Cable Insulation Applications," *IEEE Trans. Dielectr. Electr. Insul.*, vol. 22, no. 2, 2015.

[4] N. H. Rahim, K. Y. Lau, N. A. Muhamad, N. Mohamad, C. W. Tan, and A. S. Vaughan, "Structure and dielectric properties of polyethylene nanocomposites containing calcined zirconia," *IEEE Trans. Dielectr. Electr. Insul.*, vol. 26, no. 5, pp. 1541–1548, Oct. 2019.

[5] K. Y. Lau, A. S. Vaughan, G. Chen, I. L. Hosier, and A. F. Holt, "On the dielectric response of silica-based polyethylene nanocomposites," *J. Phys. D. Appl. Phys.*, vol. 46, no. 9, Mar. 2013.

[6] S. C. Tjong, G. D. Liang, and S. P. Bao, "Electrical properties of low density polyethylene/ZnO nanocomposites: The effect of thermal treatments," *J. Appl. Polym. Sci.*, vol. 102, no. 2, pp. 1436–1444, Oct. 2006.

[7] W. Cao, Z. Li, G. Sheng, and X. Jiang, "Insulating property of polypropylene nanocomposites filled with nano-MgO of different concentration," *IEEE Trans. Dielectr. Electr. Insul.*, vol. 24, no. 3, pp. 1430–1437, 2017.

[8] Y. Zhou, J. Hu, B. Dang, and J. He, "Effect of different nanoparticles on tuning electrical properties of polypropylene nanocomposites," *IEEE Trans. Dielectr. Electr. Insul.*, vol. 24, no. 3, pp. 1380–1389, 2017.

[9] J. W. Zha, J. F. Wang, S. J. Wang, Q. Qin, and Z. M. Dang, "Effect of modified ZnO on electrical properties of PP/SEBS nanocomposites for HVDC cables," *IEEE Trans. Dielectr. Electr. Insul.*, vol. 25, no. 6, pp. 2358–2365, Dec. 2018.

[10] F. Mirjalili, L. Chuah, and E. Salahi, "Mechanical and morphological properties of polypropylene/Nano α -AlComposites," *Sci. World J.*, vol. 2014, pp. 1–13, 2014.

[11] J.-W. Zha, Q.-Q. Qin, and Z.-M. Dang, "Effect of multi-dimensional zinc oxide on electrical properties of polypropylene nanocomposites for HVDC cables," *IEEE Trans. Dielectr. Electr. Insul.*, vol. 26, no. 3, pp. 868–875, Jun. 2019.

[12] I. Rytöluoto, K. Lahti, M. Karttunen, M. Koponen, S. Virtanen, and M. Pettersson, "Large-area dielectric breakdown performance of polymer films - Part II: Interdependence of filler content, processing and breakdown performance in polypropylene-silica nanocomposites," *IEEE Trans. Dielectr. Electr. Insul.*, vol. 22, no. 4, pp. 2196–2206, Aug. 2015.

[13] S. Virtanen *et al.*, "Structure and dielectric breakdown strength of nano calcium carbonate/polypropylene composites," *J. Appl. Polym. Sci.*, vol. 131, no. 1, Jan. 2014.

[14] F. W. Clinard, G. F. H. Los, and L. W. Hobbs, "Neutron irradiation damage in MgO, Al2O3 and MgAl2O4 ceramics," *J. Nucl. Mater.*, vol. 108, pp. 655–670, 1982.

[15] A. Samad, K. Y. Lau, I. A. Khan, A. H. Khoja, M. M. Jaffar, and M. Tahir, "Structure and breakdown property relationship of polyethylene nanocomposites containing laboratory-synthesized alumina, magnesia and magnesium aluminate nanofillers," *J. Phys. Chem. Solids*, vol. 120, pp. 140–146, Sep. 2018.

[16] M. Avella, S. Cosco, M. L. Di Lorenzo, E. Di Pace, M. E. Errico, and G. Gentile, "Nucleation activity of nanosized CaCO3 on crystallization of isotactic polypropylene, in dependence on crystal modification, particle shape, and coating," *Eur. Polym. J.*, vol. 42, no. 7, pp. 1548–1557, Jul. 2006.

[17] J. Junges, A. J. Zattera, L. S. Lima, L. B. Gonella, J. Junges, and A. J. Zattera, "Influence of Different Nanofillers on The Thermal and Mechanical Properties of Polypropylene," in *Proceedings of the Polymer Processing Society 29th Annual Meeting*, 2013.

[18] F. Morel, V. Bounor-Legaré, E. Espuche, O. Persyn, and M. Lacroix, "Surface modification of calcium carbonate nanofillers by fluoro- and alkyl-alkoxysilane: Consequences on the morphology, thermal stability and gas barrier properties of polyvinylidene fluoride nanocomposites," *Eur. Polym. J.*, vol. 48, no. 5, pp. 919–929, May 2012.

[19] Z. Lin, Z. Huang, Y. Zhang, K. Mai, and H. Zeng, "Crystallization and Melting Behavior of Nano-CaCO 3 /Polypropylene Composites Modified by Acrylic Acid," 2003.

[20] [20] M. Y. A. Fuad, H. Hanim, R. Zarina, Z. A. M. Ishak, and A. Hassan, "Polypropylene/calcium carbonate nanocomposites - effects of processing techniques and maleated polypropylene compatibiliser," *Express Polym. Lett.*, vol. 4, no. 10, pp. 611–620, Oct. 2010.

[21] W. Guo, B. Han, and Z. Li, "DC voltage current characteristic of Silicon Carbide/ low-density polyethylene composites," in *2010 International Forum on Strategic Technology, IFOST 2010*, 2010, pp. 365–368.

[22] N. H. Rahim, K. Y. Lau, N. A. Muhamad, N. Mohamad, W. A. W. A. Rahman, and A. S. Vaughan, "Effects of filler calcination on structure and dielectric properties of polyethylene/silica nanocomposites," *IEEE Trans. Dielectr. Electr. Insul.*, vol. 26, no. 1, pp. 284–291, Feb. 2019.